CRAB CROSSING FOR LHC UPGRADE *

Rama Calaga
Brookhaven National Lab, Upton, NY

Abstract

The LHC luminosity upgrade aims at reducing the collision point betas by a factor of 2-3 of the design value. Consequently the Piwinski angle is increased well beyond 1 to keep a normalized beam separation in the common focusing channels, thus diminishing the benefit of the beta* reduction. Crab cavities will not only recover this luminosity loss but also enable luminosity leveling, a vital ingredient for the upgrade. The baseline scenario for a crab crossing implementation in the LHC, primarily focusing on the RF cavity development is presented. Constraints from aperture, impedance and machine protection are also highlighted.

INTRODUCTION

The LHC interaction region (IR) employs a common focusing channel for both beams. Due to the 25ns bunch spacing, the two beams encounter each other in 36 places on the left and the right of the collision point. Therefore, a crossing angle is induced to physically separate the beams to about 10σ to avoid the parasitic encounters. The luminosity upgrade of the LHC aims to squeeze the collision point β^* by factor of 2-3 below the design value. Table 1 shows some relevant parameters for the nominal and subsequent upgrade of the LHC.

Table 1: Relevant LHC nominal and upgrade parameters.

	Unit	Nominal	Upgrade
Energy	[TeV]	3.5-7	7
Protons/Bunch	[10^{11}]	1.15	1.7
Average current	[Amps]	0.58	0.86
Bunch Spacing	[ns]	50-25	25
ϵ_n (x,y)	[μm]	2-3.75	
σ_z (rms)	[cm]	7.55	7.55
$IP_{1,5}$ β^*	[cm]	55-150	15-25
Betatron Tunes	{Qx, Qy}	{64.31, 59.32}	
Rev. Freq	kHz	11.245	
Piwinski Angle	Φ	0.64	1.1-1.4
Peak luminosity	[$x10^{34}$cm^{-2}s^{-1}]	0.1-1	5

This requires an increase in the crossing angle to maintain the normalized beam to beam separation near the IR. Consequently the effective luminosity gain is reduced due to the larger crossing angle given by

$$L \approx L_{\circ}.\left(1+\Phi^2\right)^{-1/2} \quad (1)$$

where $\Phi = \sigma_z\theta_c/\sigma_x^*$ is the Piwinski angle. For Φ sufficiently large (see Tab. 1), the luminosity reduction becomes large.

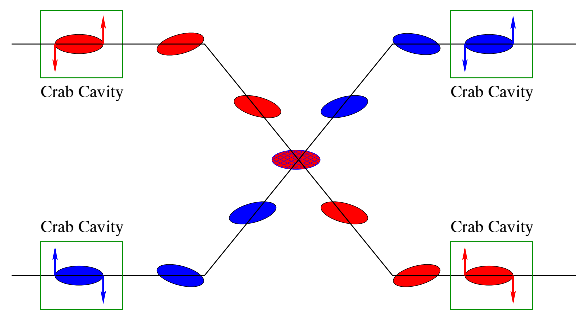

Figure 1: Concept of crab crossing scheme using RF cavities to maximize the bunch overlap at the collision points.

To fully exploit the beam size reduction a compensation of the crossing angle and in addition leveling of luminosity with crab cavities (see Fig. 1) is required [1, 2, 3]. In addition, the crab cavities offer a natural luminosity leveling knob to maximize the integrated luminosity and the lifetime of the IR magnets due to radiation damage. This paper will describe the present status of the crab project and forthcoming R&D focusing on superconducting deflecting cavities.

LAYOUT & SPECIFICATIONS

A local crab scheme (see Figure 2) where the cavities are placed in the interaction region offers the most flexibility in optics and satisfy the alternating crossing schemes as in IP_1 & IP_5.

A draft optics (Ref. [4]) to reach the desired low beta (15cm) for the upgrade with approximately 10m of physical space to accommodate the crab cavities within the interaction region is depicted in Fig. 3. The cavities are placed between the D_2 separation dipole and insertion quadrupole Q_4 which is presently the closest location to the collision point while the beams being completely separated.

The cavity voltage required for each scenario can be calculated using

$$V_{crab} = \frac{2cE_0 \tan{(\theta_c/2)}\sin{(\mu_x/2)}}{\omega_{RF}\sqrt{\beta_{crab}\beta^*}\cos{(\psi^x_{cc\rightarrow ip}-\mu_x/2)}} \quad (2)$$

* This work partially supported by the US Department of Energy through the LARP program.

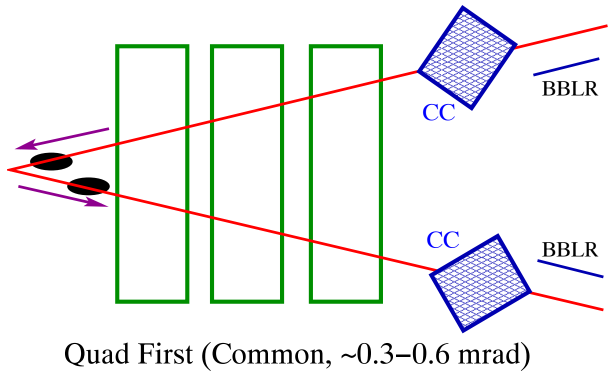

Figure 2: Schematic of the LHC interaction region with common focusing channels and independent crab cavities in a local scheme placed after the beams are separated.

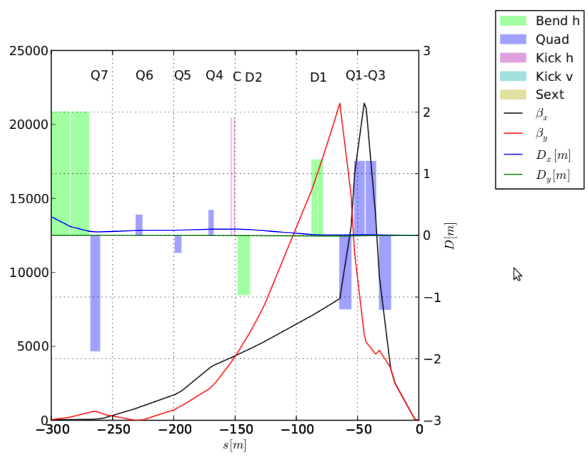

Figure 3: Draft optics and magnetic elements in the IR_1 and IR_5 region for the LHC upgrade with $\beta^* = 15\text{cm}$ [4]. The pink blocks represent the potential location ($\sim$10 m) for cavities.

where E_0 is the beam energy, ω_{RF} is the RF frequency of the cavity, β_{crab} and β^* are the beta-functions at the cavity and the IP respectively, $\psi^x_{cc\rightarrow ip}$ is the phase advance from the cavity to the IP and μ_x is the betatron tune.

Superconducting RF is the technology choice to reach required high transverse kick voltages. The primary specifications taking into account the optics, technology and physical constraints are listed in Table 2

Due to the long bunch length, the RF frequency is chosen to be within the range of 400-800 MHz with 400 MHz being the baseline. However, the spacial constraints in the interaction regions make it incompatible for conventional elliptical cavity even at 800 MHz due to their transverse size. Therefore, new design concepts with a compact footprint are essential (see Table 2).

Table 2: Specifications for crab cavities in IR_1 and IR_5 high luminosity regions for a local scheme.

	Unit	Value
Frequency	MHz	400.8
# of Cavities/IP	-	8
V_T (/Cavity)	MV	5.0
E_{Peak}	MV/m	< 45
B_{Peak}	mT	< 80
Beam pipe radius	mm	42
Cav outer Envelope	mm	<150
Module Length	m	< 1
IP β^*	cm	15
β_{crab}	km	$\sim$5
Non-linear harmonics	$\times 10^{-4}$	2-3

IMPEDANCE & RF TECHNOLOGY

The LHC impedance is dominated by the numerous collimators but additional impedance (both narrow band and broadband) from sources like crab cavities need to be minimized. It is estimated that single and coupled-bunch longitudinal modes above 2 GHz will be Landau-damped due to the frequency spread of synchrotron oscillations.

Impedance Budget

Tolerances can be set by estimating the impedance requirements given by [5],

$$R_{sh,L} < \frac{\eta E}{eI_0\beta^2}\left(\frac{\Delta}{E}\right)^2 \frac{\Delta\omega_s}{\omega_s}\frac{F}{f_0\tau}G(f_r\tau) \quad (3)$$

$$Im\left(\frac{Z}{n}\right) < \frac{\eta E}{eI_b\beta^2}\left(\frac{\Delta}{E}\right)^2 \frac{\Delta\omega_s}{\omega_s}f_0\tau. \quad (4)$$

In the transverse plane the natural frequency spread, chromaticity, bunch-by-bunch transverse damper and Landau octupoles should also damp potentially unstable modes above 2 GHz. The stability limit from Landau octupoles at 7 TeV can be formulated in terms of a maximum limit on tune shifts ($\text{Re}\{\Delta Q\} < 3\times 10^{-4}$, $\text{Im}\{\Delta Q\} < 1\times 10^{-4}$). Pessimistically assuming that the sampling frequency falls on the resonance,

$$R_{sh,T} \ll \frac{Z_0 C\gamma}{r_0 M N_b \beta}\left|Im\{\Delta Q\}\right|_{max} \quad (5)$$

An additional factor of $\beta/\langle\beta\rangle$ is needed to account for the local β-function. In the longitudinal plane, impedance threshold is defined by the anticipated 200 MHz RF system at 450 GeV. In the transverse plane, the threshold is given by the damping time at 450 GeV from the bunch by bunch feedback system. Table 3 lists the thresholds both for longitudinal and transverse planes for nominal intensities. These values are reduced by up to a factor of 2 for upgrade intensities of 1.7×10^{11} p/bunch.

Table 3: Impedance thresholds at 450 GeV and 7 TeV in the LHC.

Parameter	Unit	Long		Trans
		Inj	Top	
Coup bunch, R_{sh}	kΩ	60	200	2.5 MΩ/m
Coup bunch, Q_{ext}		< 200		-
Broadband, Im$\{Z/n\}$	Ω	0.24	0.15	-

Cavity Geometries

The first cavity geometry originated as a two cell elliptical design at 400 MHz during the first proposal of crab crossing [6]. At this stage the conventional TM_{110} higher order mode was being employed to impart the deflecting force. Soon after, the physical constraints of the LHC became apparent and the the two-cell elliptical cavity at 800 MHz was developed as a baseline structure. 800 MHz was the highest frequency considered as RF curvature effects become non-negligible beyond this frequency and these cavities can be compatible in the IR4 region with a special dogleg. Due to tight tolerances on narrow band impedances, the cavity modes need to be strongly damped. Therefore, special coupler designs targeted at specific modes were developed [7]. Alternative damping designs were simultaneously developed for the two-cell design to meet the damping specifications [8, 13].

Due to additional additional of alternating crossing angle at two IPs and operational flexibility independent and a local crab scheme was required. A major effort to compress the cavity footprint was undertaken by a large collaboration which has recently resulted in several TEM like deflecting mode geometries (see Figure 4). Apart from being significantly smaller than its elliptical counterpart, in some designs, the deflecting mode is the primary mode thus giving paving way to a new class of cavities at lower frequencies (400 MHz) which is preferred from the RF curvature point of view (see Fig. 4).

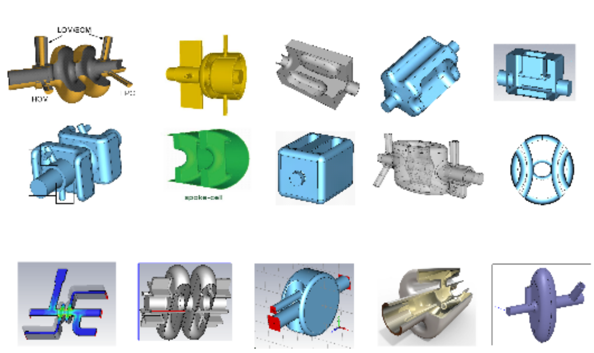

Figure 4: Design concepts explored as crab cavities for the LHC

The ratio of the kick gradient to the peak surface fields for some designs are lower by a factor of 2 or more than the elliptical counterpart. Therefore, one may theoretically expect a kick voltage also larger by a factor of 2, assuming the surface field limitations are similar to elliptical cavities. These cavities also have the added advantage of large separation in frequency between the deflecting mode and other higher order modes. Therefore, HOM damping becomes simpler.

Three primary concepts satisfying the key physical and RF constraints are being developed towards a final design (see Refs. [8, 9, 10]). Prototypes of these compact designs are underway to understand the challenges related to fabrication, surface treatment and validate the RF design to a design goal of 5 MV kick voltage per cavity module. Upon validation, a final technology choice will take place to design and construct a cryomodule hosting the prototype cavity which is foreseen to be tested in the SPS (see section).

Table 4: Three primary concepts under consideration for prototyping towards a final LHC crab cavities. Parameters are quoted for a 2.5 MV deflecting voltage.

	unit	4-rod	Modified Parallel Bar	1/4 wave
Freq	MHz	400		
E_{pk}	MV/m	33	25	45
B_{pk}	mT	49	55	110
$R/Q_{\perp}$	Ω	953	285	264
1^{st} HOM	MHz	375	619	675

CRAB CAVITY PHASE NOISE

Measurements at KEK-B show that the main frequency is modulated by discrete side bands at frequencies from 50 Hz to 32 kHz. This phase noise leads to dynamic offsets at the collision point (see Figure 5) and related emittance growth with higher frequencies being more dangerous:

$$\Delta x_{ip} = \frac{c\theta}{\omega_{RF}}\delta\phi \quad (6)$$

$$\frac{\Delta\epsilon}{\Delta t} \propto \frac{\xi^2}{\beta*}\Delta x_{ip}^2. \quad (7)$$

Dedicated noise studies were carried by inducing phase noise in the crab cavities at frequencies close to the horizontal betatron tunes and measure the corresponding beam size blow-up. The first visible effects occur at about -60dB for both rings without beam-beam which corresponds to about 0.1° RF phase noise. With beam-beam, first visible effects appear at -70dB corresponding to about 0.03° [12]. This value can be extrapolated to the LHC crab cavity tolerance as a high ceiling, i.e. the LHC cavity phase noise must be smaller than 0.03° since the radiation damping in LHC is almost negligible.

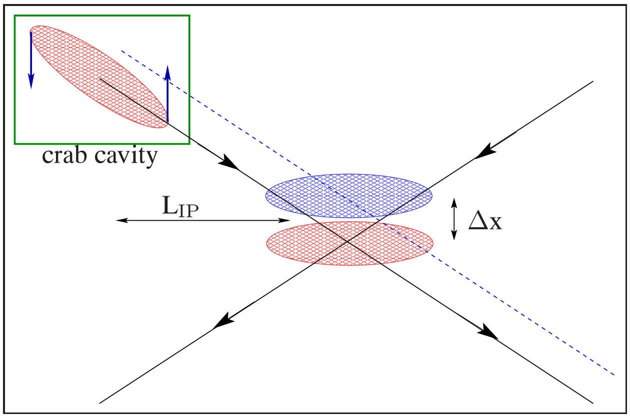

Figure 5: Schematic to illustrate offset collisions due to the crab cavity phase offset w.r.t to the beam. The blue line represents the trajectory of the offset barycenter.

Strong-strong beam-beam simulations (3D) were carried out to study phase noise effects and emittance growth of colliding beams with a local crab compensation at IP_5 in the LHC (β^*=0.25m, θ_c=0.522 mrad) [11]. The simulations were performed with 2.5 million macro-particles per beam, a 128 $\times$ 128 transverse grid, and 10 longitudinal slices with a 400 MHz local crab scheme. These simulations indicate a tolerance of $0.02\sigma\tau$ for 10% emittance growth per hour, where σ is the transverse offset and τ is the correlation time This is approximately consistent with KEK-B experiments. Weak-strong simulations with a phase error at varying frequencies observed from the KEK-B cavities [13] were performed. For the highest frequencies (32 kHz), the resulting dynamic offset collisions yield a tolerance of $\leq 0.1\sigma$ to control the emittance growth below 10% per hour. With the low-level RF technology it should be feasible to meet the tolerances but more simulations are needed to accurately define the specifications. It should be noted that the phase noise tolerances will be additionally relaxed due to luminosity leveling as the crab voltage maybe smallest when the beam-beam parameter is at a peak.

SPS AS A TEST BED

The super proton synchrotron (SPS) lends itself as an ideal test bench to study the effects of crab cavities on hadron beams and technology aspects with high intensity beams. A working group identified several aspects including integration, cryogenics, infrastructure and feasibility of a test in the SPS [14]. Fig. 6 shows the horizontal bypass in the LSS4 region currently hosting the COLDEX experiment which can be moved in only when needed. This will avoid any perturbation of regular operation of the SPS program from the crab cavity installation.

Fig. 7 shows first turn trajectories of a $1\sigma_z$ particle as a function of longitudinal position. Two collimators TCSP.51934 and a proposed test collimator from SLAC are

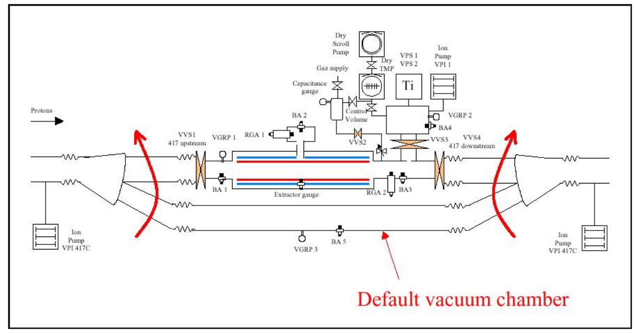

Figure 6: The LSS4 section near the COLDEX region which can host the test crab cavities in the SPS.

positioned such that one collimator sees maximum excursion while the other with almost minimum orbit deviation. This setup can aid in beam halo studies and investigate the impact on the collimator jaws.

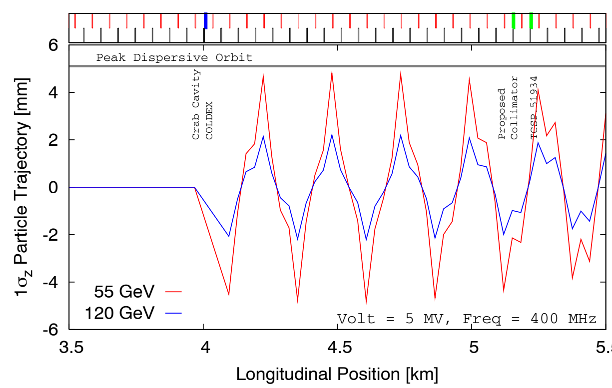

Figure 7: First turn trajectories of a particle at $1\sigma_z$ near the LSS4 region. Two collimators placed upstream are with the right phase advance to see zero and maximum orbit deviation respectively.

Three experiments (see Table 5) were performed with different energies, bunch intensities and working points to identify the dependence on the natural emittance growth to identify the optimal beam conditions for a test of crab cavities in the SPS. All experiments show emittance growths >10%/hr, the origin of which is under investigation [15]. Future experiments are planned at 270 GeV to measure the natural emittance growth. Tests at higher energy are preferred as beam studies as emittance growth from space charge and other intrinsic effects tend to decrease with energy. Therefore, the contribution solely from crab cavities can be determined. Intra-bunch orbit deviation can be detected with the existing head-tail monitor which has sub-millimeter resolution and therefore sufficient for energies $\leq$ 270 GeV.

Table 5: Beam conditions for the SPS emittance growth studies

	unit	Exp I	Exp II	Exp III
Energy	GeV	55	120	120
Intensity	x 10^{11}	1.1	0.5	0.2
# of bunches	-	1	12	1
$Q_{x,y}$	-	0.13/0.18		0.13-0.35
$\xi_{x,y}$	-	2.0		0.5
$\epsilon_{x,y}$	μm	3.1/2.8	1.5/2.0	2.5
RF Voltage	MV	3.0	2.0-4.0	4.6-6.5

MACHINE PROTECTION

Due to the immense stored energy in the LHC beams at 7 TeV (350 MJ), protection of the accelerator and related components is critical. For example, at nominal intensity and 7 TeV, 5% of a single bunch is beyond the damage threshold of the superconducting magnets [16]. Approximately, 200 interlocks with varying time constants ensure a safe transport of the beam from the SPS to the LHC and maintain safe circulating beams in the LHC. A worst case scenario for detecting an abnormal beam condition is 40 μs ($1/2$ turn), and to allow safe extraction of the beams in 3 turns [16].

Crab cavity RF failures can abruptly change the trajectories and induce unwanted beam losses. These failures can be broadly classified into two categories;

- Fast failures (single or few turns) caused by sudden cavity quench, power amplifier trips, abrupt RF phase changes due to operator errors and other hardware failures.
- Slow failures potentially caused by vacuum degradation, IR cavity to cavity voltage and phase drifts, etc..

It is of primary interest to address the case of fast failures as the potential of damage to the LHC can be significant if a large amount of the tail particles are intercepted by the machine aperture. Any crab cavity related failure must fall in the shadow of the minimum 3-turn extraction to ensure machine safety. The high Q_{ext} of the superconducting cavities could favor a slow voltage ramp down, but the voltage decay can be strongly driven by the beam. Therefore, active feedback is essential to guarantee machine protection [17].

The time-dependent beam loss distributions around the ring show that the majority of the lost particles are absorbed in the collimation system and the losses elsewhere in the ring are at the 1×10^{-6} level of the original population [18]. Figure 8 shows an example of the longitudinal pattern of the particles either lost or absorbed for a 3-turn 90° phase failure.

The SPS beam tests will investigate a multitude of aspects among which machine protection pertinent to the LHC will be of primary importance. The ultimate goal will be determine different type of interlocks based on RF (fast)

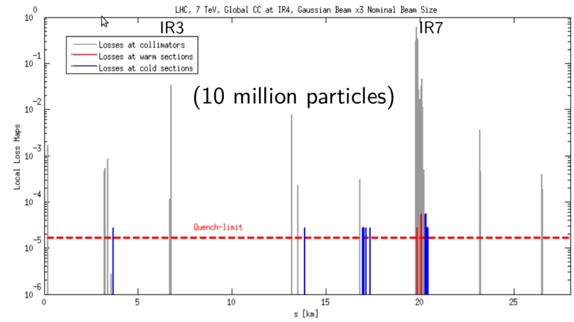

Figure 8: Longitudinal loss map for a particle distribution of $\times3$ larger beam size and a 3-turn 90° phase failure with a global crab cavity in the nominal LHC.

and orbit (slow) measurements. Cavity failure scenarios such as quench properties, cavity trips, abrupt RF voltage and phase changes and related effects on the beam will be studied. General operational aspects such as adiabatic voltage ramping, cavity transparency and other issues are also of interest.

ACKNOWLEDGMENTS

I would like to thank all the members of LHC-CC collaboration for valuable contributions and discussions. I would like to extend a special thanks to E. Ciapala, J.R. Delayen, R. deMaria, S. Fartoukh, Y. Funakoshi, E. Jensen, H.-J. Kim, N. Kota, Y. Morita, G. Burt, Z. Li, T. Sen, N. Solyak, Y. Sun, R. Tomás, J. Tuckmantel, L. Xiao, V. Yakovlev, F. Zimmermann, Advanced Energy Systems and Niowave Inc. for their contribution to the LHC studies and crab cavity development.

REFERENCES

[1] R. Calaga et al., proceedings of the Chamonix workshop, 2010.

[2] F. Zimmermann et al., proceedings of the Chamonix 2011 workshop.

[3] R. Calaga, S. Myers, F. Zimmermann, LHC-CC10 Summary report, 2011.

[4] R. deMaria, S. Fartoukh, presented at the LHC-CC10, CERN, Geneva, 2010.

[5] E. Shaposhnikova, LHC Project Note 242 (2000); E. Shaposhnikova, LHC-CC10, CERN, Geneva, 2010.

[6] R. Calaga et al., in the proceedings of the CARE-HHH 2006, Valencia, 2006.

[7] L. Xiao et al., in the proceedings of PAC09, Vancouver, Canada, 2009 (3517).

[8] G. Burt et al., presented at LHC-CC10, CERN, Geneva, 2010.

[9] J. Delayen et al., presented at LHC-CC10, CERN, Geneva, 2010; Z. Li et al., presented at LHC-CC10, CERN, Geneva, 2010.

[10] I. Ben-Zvi, presented at LHC-CC10, CERN, Geneva, 2010.

[11] K. Ohmi, Beam-beam effect with an external noise in LHC, in the proceedings of PAC09, Vancouver, Canada, 2009.

[12] R. Tomás et al., to be submitted to PRST-AB.

[13] K. Nakanishi et al, LHC-CC09, CERN, Geneva, 2010;

[14] http://emetral.web.cern.ch/emetral/CCinS/CCinS.htm.

[15] H.-J. Kim, T. Sen, CM16, Montauk, NY, 2011.

[16] R. Schmidt et al., PAC07, Albuquerque, NM, 2007; J. Wenninger, LHC-CC09, CERN, Geneva, 2009.

[17] J. Tuckmantel and E. Jensen, *private communication*.

[18] R. Calaga et al., in the proceedings of PAC11, NY, 2011.